USAXS studies of aligned samples of colloidal lamellar phases of inorganic nanosheets

Patrick Davidson[*], Christophe Penisson, Doru Constantin[*], Jean-Christophe P. Gabriel[**]

* Laboratoire de Physique des Solides, CNRS, Univ. Paris-Sud, Université Paris-Saclay, 91405 Orsay Cedex, France

[**] CEA Grenoble, Bât. C5, 17 Avenue des Martyrs, 38000 Grenoble, France

The phase diagram of colloidal suspensions of electrically charged nanosheets, such as clays, in spite of their many industrial uses, is not yet understood either experimentally or theoretically. When the nanosheet diameter is very large (~ 100 nm – 1 µm), distinguishing the lamellar liquid-crystalline phase from a nematic phase with strong stacking local order, often called "columnar" nematic, is quite challenging. Allocated beamtime allowed us to show that thanks to the newly upgraded small-angle x-ray scattering beamlines ID2 of ESRF provides high-resolution measurements which allow identifying both phases unambiguously, provided that single domains were obtained. We investigated dilute aqueous suspensions of synthetic $Sb_3P_2O_{14}^{3-}$ nanosheets that self-organize into two distinct liquid-crystalline phases, sometimes coexisting in the same sample (Figure 1). Close examination of single domain x-ray reflection profile in the directions perpendicular to the director (Figure 3B) demonstrates that these two mesophases are respectively a columnar nematic (Figure 2A) and a lamellar phase (Figure 2B). In the latter, the domain size reaches up to ~ 20 µm, which means that each layer is made of τ 600 nanosheets. Since the lamellar phase was only rarely predicted in suspensions of charged disks, our results show that these systems should be revisited by theory or simulations. The unexpected stability of the lamellar phase also suggests that the rims and faces of $Sb_3P_2O_{14}^{3-}$ nanosheets may have different properties, giving them a "patchy" particle character. These results could be compared to the USAXS patterns obtained in the case of clays (Beidellite for example, Figure 2C) which present a typical columnar nematic phase.

These findings were published in the *Proceeding of the National Academy of Sciences* 2018, 115 (26) pp. 6662-6667.

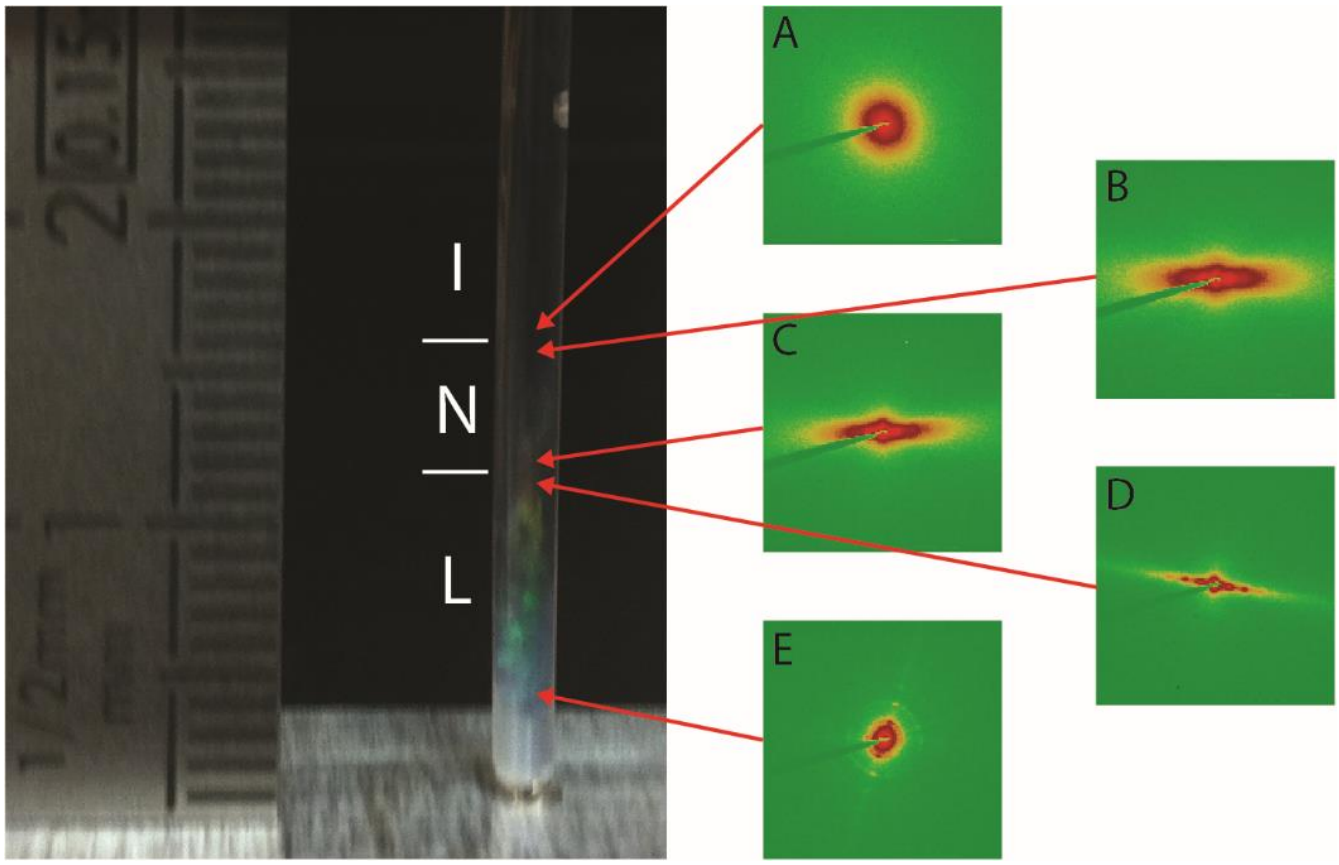

Figure 1: A 2-mm diameter X-ray capillary was scanned from bottom to top, every 0.2 mm on the SWING SAXS beamline. Typical patterns are displayed: A) isotropic phase just above the I – N interface; B) nematic phase just below the I-N interface & C) just above the N – L interface; D) lamellar phase just below the N-L interface & E) in the middle of the lamellar phase region.

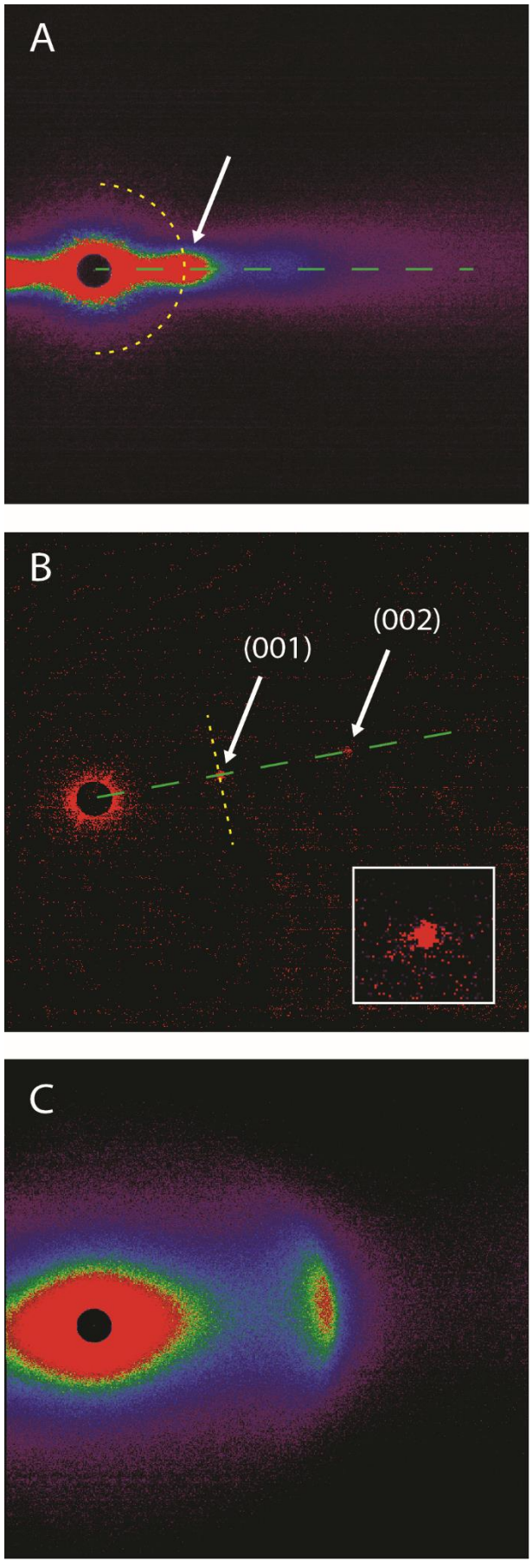

Figure 2 (to the left): High-resolution SAXS patterns recorded at the ID02 beamline of ESRF of: $H_3Sb_3P_2O_{14}$ nanosheet suspensions in A) the nematic phase (Size B, $\phi = 0.13‰$, image 1083); B) the lamellar phase (Size C, $\phi = 0.21‰$, image # 300) (The bottom right inset is a magnified portion of the pattern showing the (001) reflection.); and C) the nematic phase of a beidellite clay suspension (<D> = 280 nm, $\phi = 0.8\%$). In A) and B), the green dashed lines show the radial cuts through the patterns used to obtain the radial profiles of scattered intensity, the yellow dotted half-circle in A) shows the cut used to obtain the azimuthal profile and hence the nematic order parameter, and the yellow dotted line in B) shows the cut used to obtain the transverse profile of the lamellar reflection.

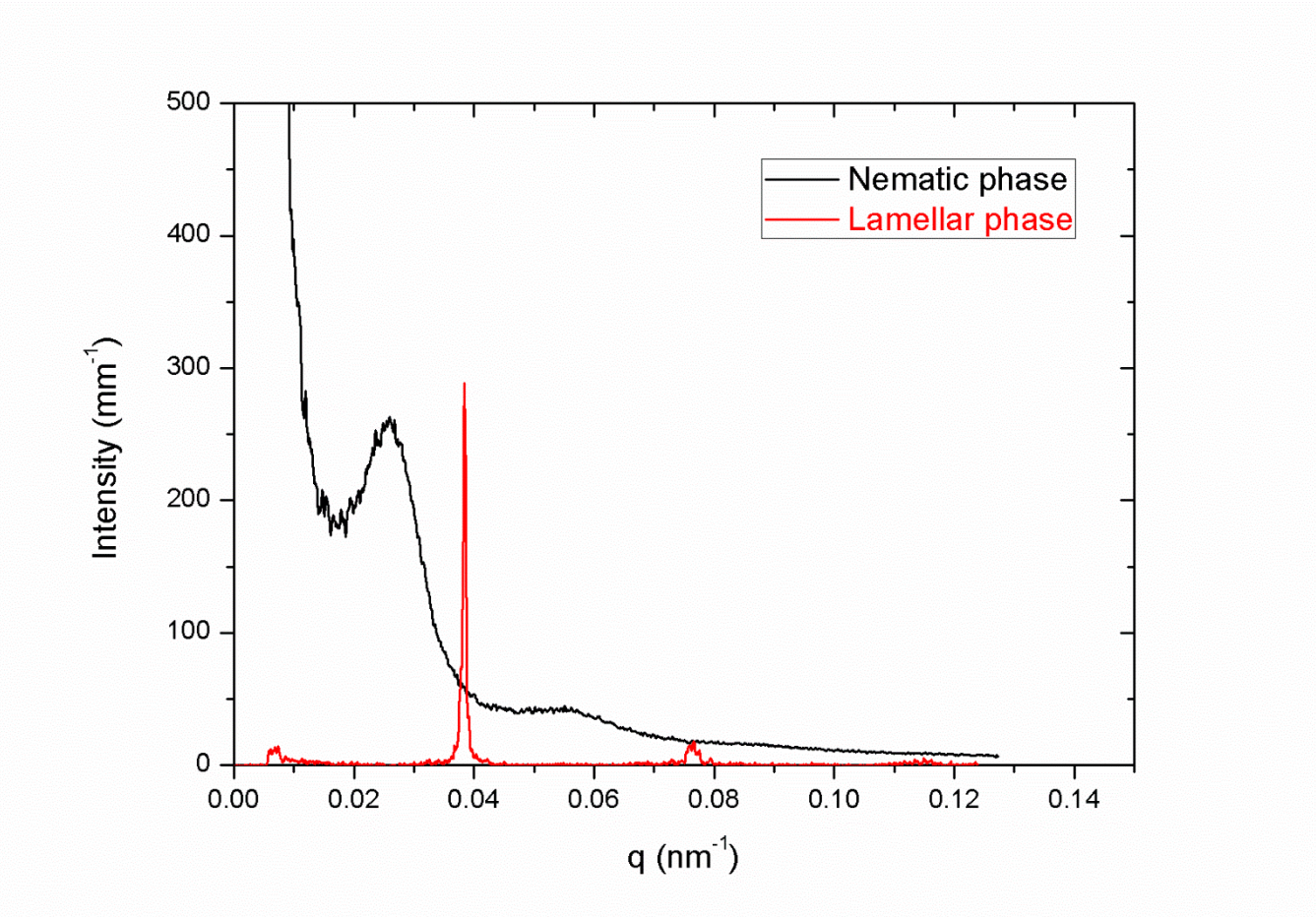
Nematic phase
Lamellar phase
Intensity (mm^{-1})
q (nm^{-1})
0
100
200
300
400
500
0.00
0.02
0.04
0.06
0.08
0.10
0.12
0.14

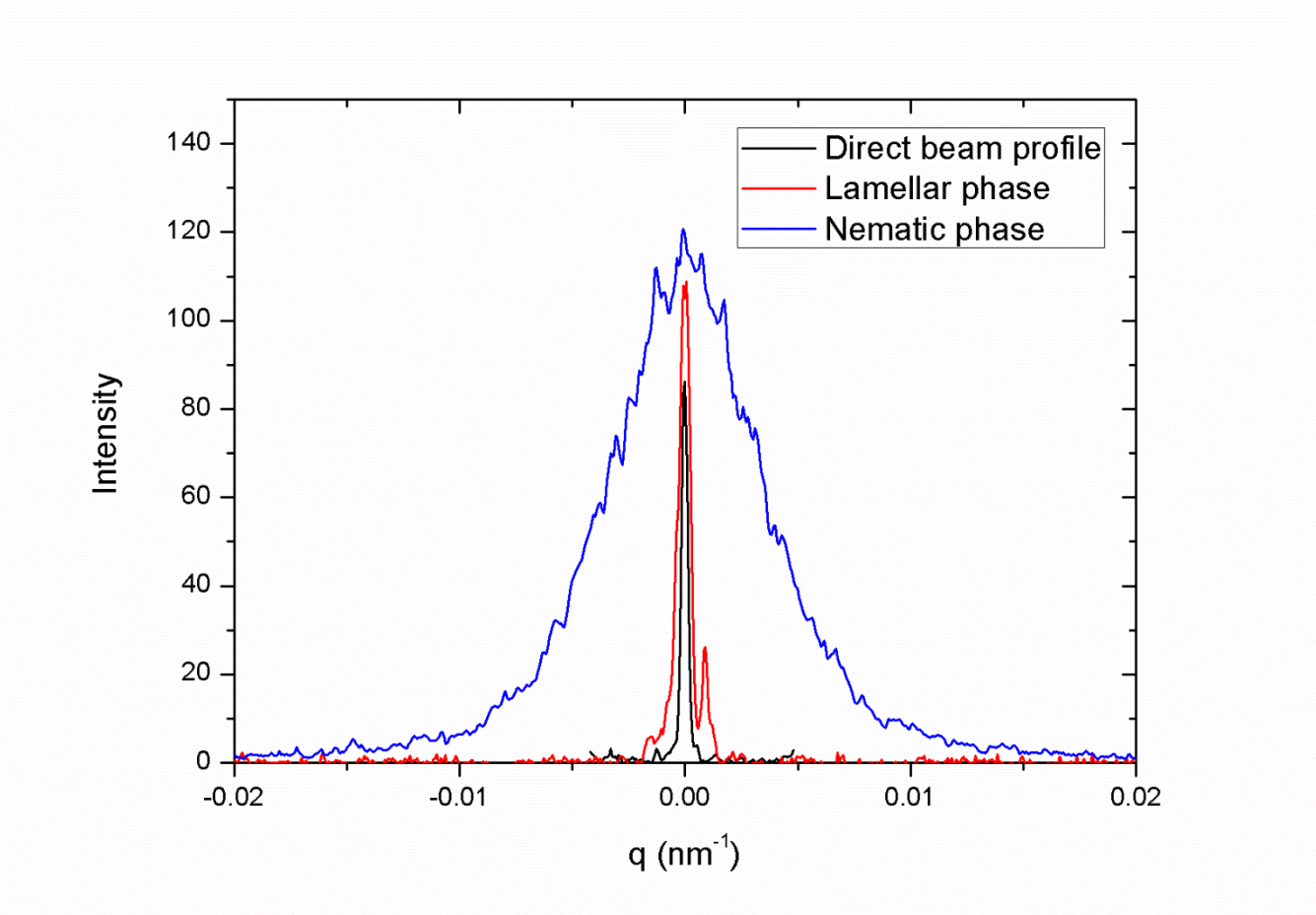

Figure 3: A) Radial profiles of scattered intensity drawn from the high-resolution SAXS patterns of the nematic and lamellar phases shown in Figure 5. (The scattered intensity of the nematic phase has been divided by 2 for easier comparison.); B) Transverse profiles drawn from the same scattering patterns. (The small peak at $q_{\perp} = 10^{-3}$ nm^{-1} in the scattering from the lamellar phase is due to another small domain in the beam.)

Additionnal outcome from this beamtime allocation: In addition to this main result, this beamtime allocation also allowed us to study additional systems and namely the X-ray scattering studies of the electric field-induced orientational order in colloidal suspensions of pigment nanorods. Indeed, Under pulsed or a.c. electric fields, colloidal suspensions of nanorods can show strong electro-optic effects, such as the Kerr effect, with fast response times (a few ms), which makes them good candidates for some commercial applications. For this purpose, suspensions of Pigment red 176 nanorods in dodecane were recently developed and their physical properties have been studied. We report here on the investigation of the orientational order induced by electric fields in isotropic suspensions of pigment nanorods by three different techniques: transient electric birefringence, transient electric dichroism, and in-situ small-angle X-ray scattering under electric field ("Electro-SAXS"). We show that, in spite of the apolar character of

the solvent, the Maxwell-Wagner-O'Konski mechanism (i.e. the polarization of the counter-ion cloud around each particle) is responsible for the field-induced alignment of the nanorods. Although the particles are only weakly charged and the dielectric constant of dodecane is low, the pigment nanorods effectively behave as metallic particles in an insulating matrix and reach strong values (S ~0.5) of the induced nematic order parameter at moderate field amplitudes (~1 V/μm). This study confirms the feasibility of using suspensions of Pigment red nanorods in dodecane for electrooptic applications.

These results have been published: "Optical and X-ray scattering studies of the electric field-induced orientational order in colloidal suspensions of pigment nanorods." Oleksandr Buluy, Natalie Aryasova, Oleksandr Tereshchenko, Yuriy Kurioz, Vassili Nazarenko, Alexey Eremin, Ralf Stannarius, Susanne Klein, Claire Goldmann, Patrick Davidson, Ivan Dozov, Yuriy Reznikov, *Journal of Molecular Liquids* 2018, 267, pp. 286-296 https://doi.org/10.1016/j.molliq.2018.02.003.